ELSEVIER

Journal of Alloys and Compounds 388 (2005) 109–117

Journal of ALLOYS AND COMPOUNDS

www.elsevier.com/locate/jallcom

Investigation on the characteristics of $La_{0.7}Mg_{0.3}Ni_{2.65}Mn_{0.1}Co_{0.75+x}$ (x = 0.00–0.85) metal hydride electrode alloys for Ni/MH batteries Part II: Electrochemical performances

Yongfeng Liu, Hongge Pan*, Mingxia Gao, Rui Li, Xianzhong Sun, Yongquan Lei

Department of Materials Science and Engineering, Zhejiang University, Hangzhou 310027, People's Republic of China

Received 8 June 2004; received in revised form 6 July 2004; accepted 6 July 2004

Abstract

In this paper, the electrochemical performances of the $La_{0.7}Mg_{0.3}Ni_{2.65}Mn_{0.1}Co_{0.75+x}$ (x = 0.00–0.85) alloy electrodes were studied. The results show that, with increasing amount of Co addition, the maximum discharge capacities of the alloys decrease monotonously due to the relative change of the phase abundance of the (La, Mg)Ni_3 phase and the $LaNi_5$ phase coexisting in the alloys and the increase of the equilibrium pressure for hydrogen desorption. Moreover, the cycling stability of the alloy electrodes was noticeably improved with increasing Co addition because of the relatively lower value of V_H and the formation of protective oxides (hydroxides). The high rate dischargeability of the alloy electrodes increases first and then decreases with increasing amount of Co addition, and the alloy electrode with x = 0.30 exhibits the best electrochemical kinetics. In addition, the electrochemical kinetic parameters study, including the charge-transfer resistance at the surface R_{ct}, the polarization resistance R_p, the exchange current density I_0, the limiting current density I_L and the diffusion coefficient of hydrogen in the alloys D, also confirm this result.

Keywords: Hydrogen storage alloys; Ni/MH batteries; Electrochemical reactions; Cyclic stability; Electrochemical kinetics

1. Introduction

In part I [1], the phase structures and hydrogen storage properties of the $La_{0.7}Mg_{0.3}Ni_{2.65}Mn_{0.1}Co_{0.75+x}$ (x = 0.00–0.85) hydrogen storage alloys have been systematically investigated and reported. In this paper (part II), the electrochemical performances were studied systematically and the correlation between the electrochemical performances and the phase structures were discussed. Previously, the functions of partial substitution of Co for Ni in the rare earth-based hydrogen storage alloys were extensively studied and attracted attention in practical and scientific meanings. Willems and Buschow [2] reported that the stability of $LaNi_{5-x}Co_x$ (x = 1–5) hydrogen storage alloys was markedly improved by increasing the Co content in the alloys with less discharge capacity loss, because the molar volume of hydrogen (V_H) in the hydride phase was depressed, which reduces the lattice expansion and the stress cracking. Adzic and co-workers [3] indicated that another role of Co in the rare earth-based alloys was an increase of the surface passivation owing to the increase of the oxide coverage on the cycled alloy and a subsequent increase of stability due to the diminution of the exposure of the active material to the alkaline electrolyte. Moreover, Chartouni et al. [4] revealed the alloys with Co exhibited lower the Vickers hardness, which also may be beneficial for the enhancement of stability over repeated charge/discharge cycles. All the above phenomena indicate that the presence of Co is very efficient for increasing the cyclic stability of the rare earth-based hydrogen storage alloys. Therefore, it is expected that the cyclic stability of the new type La–Mg–Ni–Co alloys can be also obviously improved and is finally close to the level of the practical application by increasing the content of Co. Moreover, in the previous study of the rare earth-based hydrogen storage alloys, only the effects of partial

* Corresponding author. Tel.: +86-571-8795-2576; fax: +86-571-8795-1152.
E-mail address: honggepan@zjuem.zju.edu.cn (H. Pan).

0925-8388/$ – see front matter © 2004 Elsevier B.V. All rights reserved.
doi:10.1016/j.jallcom.2004.07.014

substitution of Co for Ni were reported, however, the investigations of the nonstoichiometric addition of Co in B-site of the alloys have not yet been carried out.

In the present study, the content of Co was increased by adding more Co to the B-site of the $La_{0.7}Mg_{0.3}Ni_{2.65}Mn_{0.1}Co_{0.75}$ alloys, and then the electrochemical performances of the $La_{0.7}Mg_{0.3}Ni_{2.65}Mn_{0.1}Co_{0.75+x}$ (x = 0.00, 0.15, 0.30, 0.40, 0.55, 0.70, and 0.85) alloys, including activation, the discharge capacity, the cyclic behavior, the high rate dischargeability (HRD), the electrochemical impedance spectroscopy (EIS), the exchange current density I_0, the limiting current density I_L and the hydrogen diffusion coefficient D were systematically studied and reported.

2. Experimental details

The $La_{0.7}Mg_{0.3}Ni_{2.65}Mn_{0.1}Co_{0.75+x}$ (x = 0.00, 0.15, 0.30, 0.40, 0.55, 0.70, and 0.85) alloys were prepared as described in part I [1]. For electrochemical measurements, part of the alloy samples were mechanically crushed and ground to powder below 300 mesh. The average particle diameter of the resulting powder as measured by a Malvern particle analyzer Mastersizer2000 is 26.24 μm.

Each test electrode was prepared by mixing 100 mg specific alloy powders with carbonyl nickel powder in a weight ratio of 1:4 and then the mixture was cold-pressed into a pellet under a pressure of 16 MPa. The electrochemical properties of each alloy sample (used as the negative electrode) were measured in a tri-electrode open system with a sintered $Ni(OH)_2$/NiOOH positive counter electrode and a Hg/HgO reference electrode. The electrolyte is 6 M KOH solution. For activation and charge/discharge cycling, each electrode was charged at 100 mA/g for 5 h followed by a 10 min rest and then discharged at 60 mA/g to the cut-off potential of −0.6 V versus the Hg/HgO reference electrode. To compare the high rate dischargeability of the alloy electrodes, the discharge capacities at several specific discharge current densities were measured. Electrochemical impedance spectroscopy (EIS) studies were conducted at 50% depth of discharge (DOD) using a Solartron SI1287 Electrochemical Interface with 1255B Frequency Response Analyzer, using the ZPLOT electrochemical impedance software. Before the EIS measurements, the electrodes were first completely activated by charging/discharging for 5 cycles. The EIS spectra of the electrodes were obtained in the frequency range from 10 kHz to 5 mHz with an ac amplitude of 5 mV under the open-circuit condition. The micro-polarization curves and Tafel polarization curves of the electrodes were measured on Solartron SI1287 potentiostat (using the CorrWare electrochemistry/corrosion software) by scanning the electrode potential at a rate of 0.1 mV/s from −5 to 5 mV (versus open circuit potential) and 5 mV/s from −500 to 1500 mV (versus open circuit potential) at 50% depth of discharge (DOD), respectively. The hydrogen diffusion coefficient was estimated by the potential-step method, and the experiments were carried out on a Solartron SI1287 potentiostat (using the CorrWare electrochemistry/corrosion software) at 100% charge state. An overpotential of +600 mV was applied and the discharge time is 5000 s.

3. Results and discussion

3.1. Discharge capacities and cyclic behavior

Fig. 1 shows the maximum discharge capacities of the $La_{0.7}Mg_{0.3}Ni_{2.65}Mn_{0.1}Co_{0.75+x}$ (x = 0.00–0.85) alloy electrodes with various Co additions at a discharge current density of 60 mA/g, which are also listed in Table 1. As shown in Fig. 1 and Table 1, it is very obvious that, with increasing amount of Co addition, the maximum discharge capacities of the alloys decrease monotonously from 403.0 mAh/g (x = 0.00) to 261.7 mAh/g (x = 0.85). This result can be attributed to the relative change of the phase abundance of the (La, Mg)Ni_3 phase and the $LaNi_5$ phase coexisting in the alloys studied. In part I [1], it was found that the phase content of the (La, Mg)Ni_3 phase was decreased and that of the $LaNi_5$ was increased progressively with an increase in the amount of Co addition. Moreover, Oesterreicher et al. [5] and Takeshita et al. [6] have reported that the hydrogen storage capacity of $LaNi_3$ with $PuNi_3$-type structure is larger than that of the $LaNi_5$ alloys. So the decrease of the (La, Mg)Ni_3 phase and the increase of the $LaNi_5$ phase here are believed to be one of reasons for the decrease in discharge capacities of the alloys studied. Another reason for the decrease in the discharge capacity is thought to be associated with the increase in the equilibrium pressure for hydrogen desorption. As observed in part I [1], the cell volumes of both the (La, Mg)Ni_3 phase and the $LaNi_5$ phase were compressed due to Co addition, which induces an increase in the equilibrium pressure for hydrogen absorption/desorption and a subsequent reduction of the available hydrogen storage capacity. This phenomenon also contributed to the decrease in the discharge capacities of the alloys with higher Co addition.

Fig. 2 illustrates the cyclic life curves of the $La_{0.7}Mg_{0.3}Ni_{2.65}Mn_{0.1}Co_{0.75+x}$ (x = 0.00–0.85) alloy electrodes at 303 K. Table 1 also lists the number of activa-

Table 1
Electrochemical characteristics of the $La_{0.7}Mg_{0.3}Ni_{2.65}Mn_{0.1}Co_{0.75+x}$ (x = 0.00–0.85) alloy electrodes

x	C_{max} (mAh/g)	N_a[a]	C_{110}/C_{max} (%)	HRD_{1750}[b] (%)
0.00	403.0	2	30.5	56.3
0.15	390.0	2	36.6	58.1
0.30	354.4	1	38.5	61.4
0.40	323.2	2	42.3	50.2
0.55	284.8	2	51.4	44.9
0.70	264.2	2	60.4	38.7
0.85	261.7	2	62.4	32.3

[a] The cycle numbers needed to activate the electrodes.
[b] The high rate dischargeability with discharge current density I_d = 1750 mA/g.

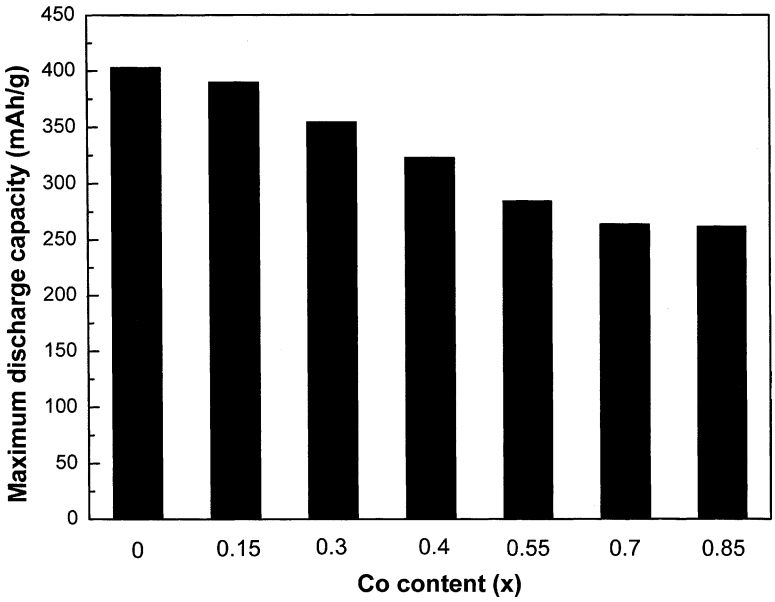

Fig. 1. The maximum discharge capacities of the $La_{0.7}Mg_{0.3}Ni_{2.65}Mn_{0.1}Co_{0.75+x}$ (x = 0.00–0.85) alloy electrodes at 303 K.

tion cycles for fully activating the alloy electrodes. It can be seen that these alloys can be easily activated to their maximum discharge capacities within two cycles, which is very beneficial to their practical application. Moreover, it is interesting to note that the cyclic stability of the alloy electrodes was noticeably improved with increasing the amount of Co addition. Fig. 3 shows the discharge capacity retention of the $La_{0.7}Mg_{0.3}Ni_{2.65}Mn_{0.1}Co_{0.75+x}$ (x = 0.00–0.85) alloy electrodes after different charge/discharge cycles at 303 K, where C_{max}, C_{30}, C_{60}, C_{90}, C_{110} are the maximum discharge capacity, the discharge capacity of the 30th, 60th, 90th, and 110th cycle, respectively. It is very obvious that, after 110 charge/discharge cycles, the discharge capacity retention of the alloy electrodes was increased from 30.5 (x = 0.00) to 62.4% (x = 0.85). It is well known that the capacity decay of metal-hydride electrodes is primarily determined by two factors, surface passivation owing to surface oxides and/or hydroxides and the molar volume of hydrogen, V_H, in the hydride phase [2,7]. Thus, in this study, the effective improvement of the cyclic stability of the alloy electrodes with higher Co addition can be mainly attributed to the relatively lower value of V_H as reported by Willems and Buschow [2]. On the other hand, the formation of protective oxides (hydroxides) may also contribute to their lower capacity decay [3]. Moreover, for the alloy with a given composition, the value of C_{30}/C_{max} is lower than that

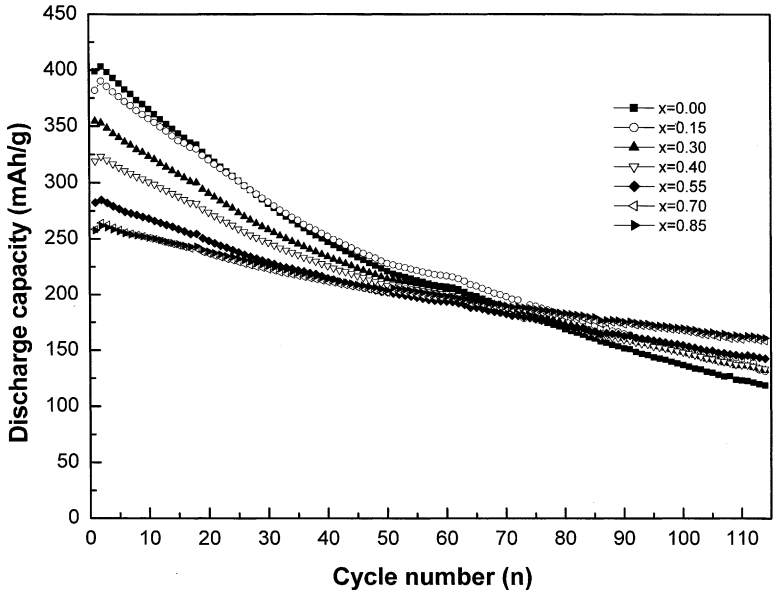

Fig. 2. The cyclic stability curves of the $La_{0.7}Mg_{0.3}Ni_{2.65}Mn_{0.1}Co_{0.75+x}$ (x = 0.00–0.85) alloy electrodes at 303 K.

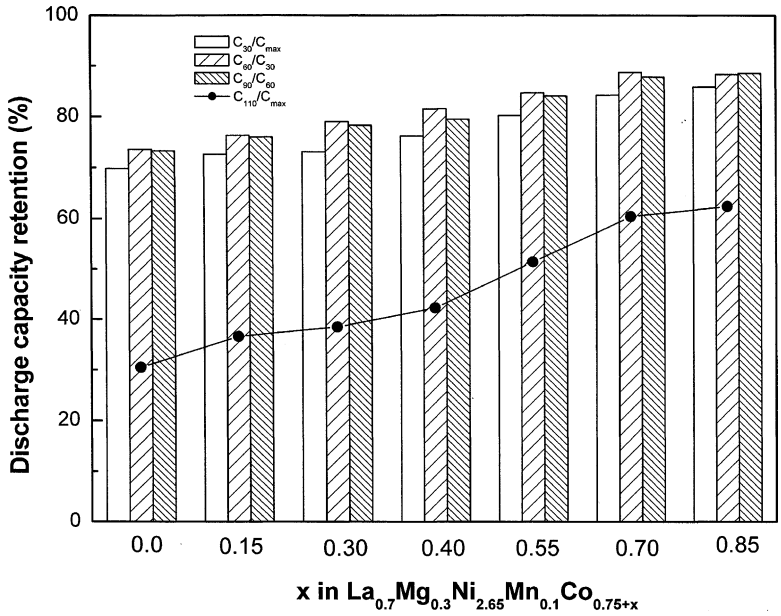

Fig. 3. The discharge capacity retention of the $La_{0.7}Mg_{0.3}Ni_{2.65}Mn_{0.1}Co_{0.75+x}$ (x = 0.00–0.85) alloy electrodes after different charge/discharge cycles at 303 K.

of C_{60}/C_{30} and C_{90}/C_{60}. For example, the C_{30}/C_{max} value for the alloy electrode with x = 0.55 is 80.2%, whereas the values of C_{60}/C_{30} and C_{90}/C_{60} increase to 84.6 and 84.0%, respectively, which indicates that Co addition can improve more effectively the latter cyclic durability of the alloy electrodes (after 30–40 charge/discharge cycles) than the former cyclic durability (before 30–40 charge/discharge cycles). This result also confirms that the discharge capacity decay of the La–Mg–Ni–Co type alloy electrodes can be distinguished into two progresses [8]. The first one is the starting 30–40 charge/discharge cycles in which the discharge capacity dropped rapidly and it may result from the corrosion of Mg in alkaline solution and the formation of a permeable $Mg(OH)_2$ film inducing the electrochemical capacity loss of the (La, Mg)Ni_3 phase and the pulverization of the alloy particles during charge/discharge cycling, and the electrochemical capacity loss of the (La, Mg)Ni_3 phase is primary reason. The other is the rest charge/discharge cycles in which the discharge capacity degradation is lower which can be attributed to the pulverization of the alloy particles and the corrosion of La in KOH solution.

3.2. High rate dischargeability

Fig. 4 illustrates the high rate dischargeability (HRD) of the $La_{0.7}Mg_{0.3}Ni_{2.65}Mn_{0.1}Co_{0.75+x}$ (x = 0.00–0.85) alloy electrodes at 303K. The HRD is calculated from the following formula:

$$\mathrm{HRD} = \frac{C_d}{C_d + C_{60}} \times 100\% \quad (1)$$

wherein C_d is the discharge capacity with a cut-off potential of −0.6 V versus Hg/HgO reference electrode at the discharge current density I_d, C_{60} is the residual discharge capacity with a cut-off potential of −0.6 V versus Hg/HgO reference electrode at the discharge current density I = 60 mA/g also after the alloy electrode has been fully discharged at the large discharge current density (I_d). It can be seen that the HRDs of the alloy electrodes were increased by adding a proper amount of Co ($x \leq 0.30$) to the $La_{0.7}Mg_{0.3}Ni_{2.65}Mn_{0.1}Co_{0.75}$ alloy, but were obviously decreased when the Co addition increases further, particularly when x reaches 0.85. Table 1 also lists the HRD of these alloy electrodes at a discharge current density of 1750 mA/g. With increasing amount of Co addition, the HRDs of the alloy electrodes increase first from 56.3 (x = 0.00) to 61.4% (x = 0.30) and then decrease sharply to 32.3% (x = 0.85). The reason for the higher HRD of the alloy electrodes with x = 0.00–0.30 may be due to the formation of a Raney Ni–Co film with higher electrocatalytic activity resulting from the concentration of Ni and Co at the alloy surface during charge/discharge cycling [9,10]. However, when x increases further, the added Co can form $Co(OH)_2$ at the alloy surface during charge/discharge cycling and increase with increasing Co addition, which decreases the rate of hydrogen desorption, and a subsequent decrease in the HRDs of the alloy electrodes with higher Co addition [11,12].

In addition, it is well known that the HRD of the hydrogen storage alloy electrodes is controlled by the electrochemical kinetics at the surface of the alloys and the diffusion rate of hydrogen in the bulk of the alloys, which are mainly determined by the charge-transfer resistance at the surface R_{ct}, the exchange current density I_0, the limiting current density I_L or the diffusion coefficient of hydrogen in the alloys D.

3.3. EIS and polarization

Fig. 5 shows the electrochemical impedance spectra (EIS) of the $La_{0.7}Mg_{0.3}Ni_{2.65}Mn_{0.1}Co_{0.75+x}$ (x = 0.00–0.85) alloy

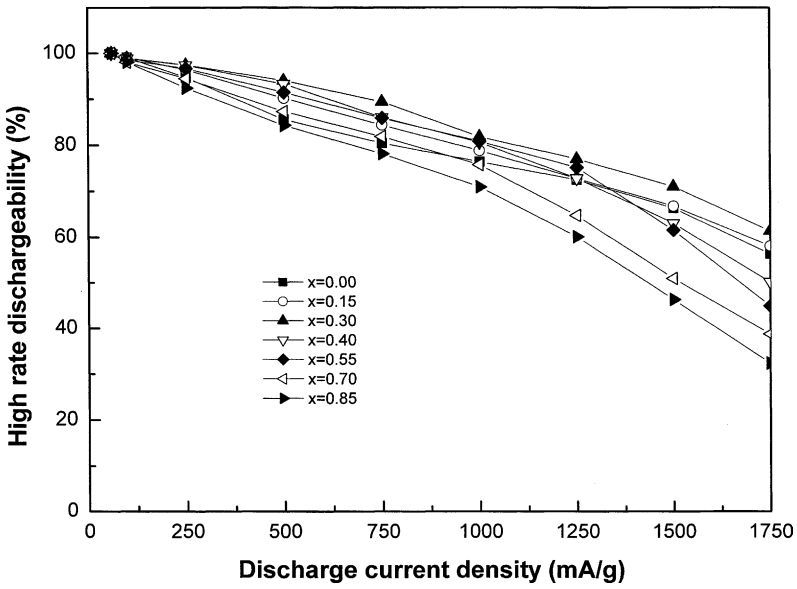

Fig. 4. High rate dischargeability (HRD) of the $La_{0.7}Mg_{0.3}Ni_{2.65}Mn_{0.1}Co_{0.75+x}$ (x = 0.00–0.85) alloy electrodes at 303 K.

electrodes at 50% DOD and 298 K. For all the alloy samples, it can be seen that the EIS spectra consist of two semicircles and a straight line. With increasing amount of Co addition, the smaller semicircle in the high-frequency region (representing the contact resistance between the alloy particles and the current collector) remains almost unchanged, but the larger semicircle in the low-frequency region (defined as a charge-transfer resistance for hydrogenation reaction) is changed, that is, the radius of the larger semicircle in the low-frequency region is decreased first and then increased with increasing amount of Co addition, which indicates that the charge-transfer resistance of the electrode surface is decreased first and then increased. The EIS data were analyzed using an equivalent circuit proposed by Kuriyama et al. [13], shown in the insert. The capacitive components labeled by C are modeled as constant-phase elements (CPE) to describe the depressed nature of the semicircles. R_{el} is ascribed to the electrolyte resistance between the MH electrode and the reference electrode. The semicircle in the high-frequency region, modeled by R_{cp} and C_{cp}, results from the contact resistance between the alloy particles and the current collector. The contact resistance and capacitance between the alloy particles generate the parameters R_{pp} and C_{pp}. R_{ct} and C_{ct}, representing the semicircle in the low-frequency region contribute to the charge-transfer reaction resistance and the double-layer capacitance, respectively. R_w is the Warburg impedance. The

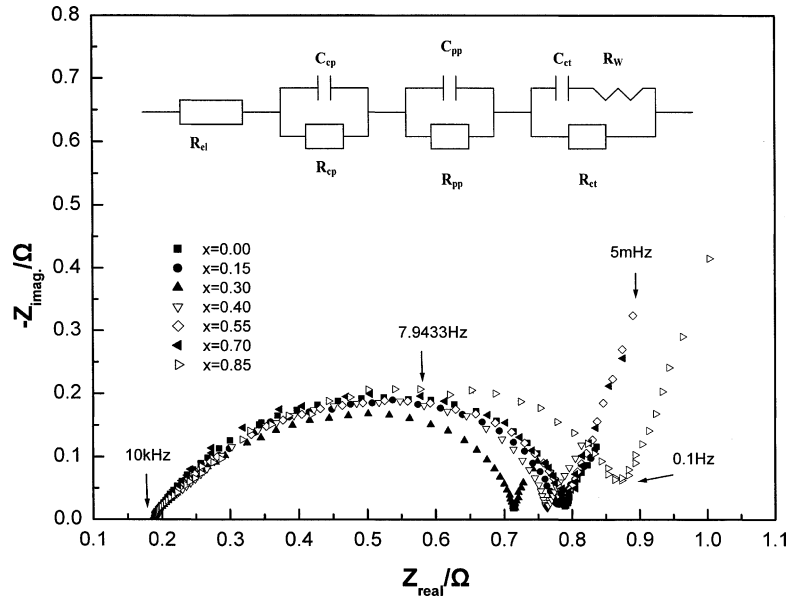

Fig. 5. Electrochemical impedance spectra (EIS) of the $La_{0.7}Mg_{0.3}Ni_{2.65}Mn_{0.1}Co_{0.75+x}$ (x = 0.00–0.85) alloy electrodes at 50% DOD and 298 K.

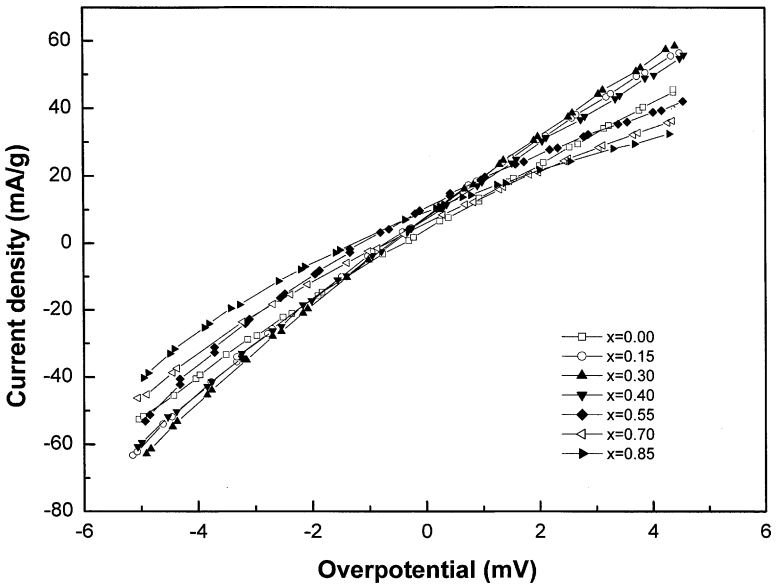

Fig. 6. Micro-polarization curves of the $La_{0.7}Mg_{0.3}Ni_{2.65}Mn_{0.1}Co_{0.75+x}$ (x = 0.00–0.85) alloy electrodes at 50% DOD and 298 K.

parameters in the equivalent circuit were calculated by a nonlinear least squares fit using the ZView electrochemical impedance software, and the charge-transfer reaction resistance R_{ct} of the alloy electrodes is summarized in Table 2. It is obvious that, with increasing Co addition, the R_{ct} values decrease first form 50.5 mΩ (x = 0.00) to 35.4 mΩ (x = 0.30) and then increase to 63.3 mΩ (x = 0.85). This result suggests that the reaction of hydrogen at the surface of the alloys changes first more easily when x increases from 0.00 to 0.30, which can be attributed to the presence of a Ni–Co network with high electrocatalytic activity owing to the concentration of Co and Ni [9,10]. And then, with further increasing x, the reaction of hydrogen at the surface tends to become difficult, which may be the result of the formation and increase of $Co(OH)_2$ at the alloy surface causing a surface passivation with increasing Co addition [11,12].

Fig. 6 shows the micro-polarization curves of the $La_{0.7}Mg_{0.3}Ni_{2.65}Mn_{0.1}Co_{0.75+x}$ (x = 0.00–0.85) alloy electrodes at 50% DOD and 298 K. It can be noted that, when the overpotential is changed within a small range (± 5 mV), there is a good linear dependence between the current and overpotential. From the slope of the corresponding micro-polarization curve, the polarization resistance R_p of the alloy electrode studied can be obtained and has been listed in Table 2. When increasing the amount of Co addition, the R_p values of the alloy electrodes decrease first from 97.3 (x = 0.00) to 78.3 mΩ (x = 0.30) and then increase to 127.8 mΩ (x = 0.85), which is consistent with the EIS measurement and also indicates that the reaction rate of hydrogen at the surface was accelerated first and then slowed down. Furthermore, it was found that the R_P values obtained from the linear polarization measurement are larger than that of the R_{ct} values obtained from the EIS measurement. The result can be explained easily because the polarization resistance R_P consists of the electrolyte resistance R_{el}, the contact resistance R_{cp} and R_{pp}, and the charge-transfer reaction resistance R_{ct}. In addition, as an important kinetic parameter responsible for the electrochemical hydrogen reaction at the surface of the alloy electrode, the exchange current density I_0 can be calculated by the following formula [14]:

Table 2
Electrochemical kinetic parameters of the $La_{0.7}Mg_{0.3}Ni_{2.65}Mn_{0.1}Co_{0.75+x}$ (x = 0.00–0.85) alloy electrodes

x	Charge-transfer reaction resistance R_{ct} (mΩ)	Polarization resistance R_p (mΩ)	Exchange current density I_0 (mA/g)	Limiting current density I_L (mA/g)	Hydrogen diffusion coefficient D ($\times 10^{-11}$cm^2/s)
0.00	50.5	97.3	264.0	1735.7	0.75
0.15	47.2	81.1	316.4	1766.8	0.80
0.30	35.4	78.3	327.8	1912.0	0.87
0.40	44.9	83.8	306.3	1653.8	0.79
0.55	55.3	103.1	249.1	1455.8	0.72
0.70	55.6	115.4	222.4	1432.3	0.65
0.85	63.3	127.8	200.8	1263.1	0.58

$$I_0 = \frac{RT}{FR_p} \quad (2)$$

where R is the gas constant, T is the absolute temperature, F is the Faraday constant and R_p is the polarization resistance. The I_0 values of the $La_{0.7}Mg_{0.3}Ni_{2.65}Mn_{0.1}Co_{0.75+x}$ (x = 0.00–0.85) alloy electrodes obtained from Eq. (2) are also tabulated in Table 2. It can be seen that the I_0 values of the alloy electrodes increase first from 264.0 (x = 0.00) to 327.8 mA/g (x = 0.30) and then decrease to 200.8 mA/g (x = 0.85) with increasing amount of Co addition. When x increases from 0.00 to 0.85, the I_0 values of the alloy electrodes increase, which can be attributed to the fact that Co and Ni became concentrated at the surface of the alloys and formed a Raney Ni–Co film with higher electrocatalytic activity after proper Co addition [9,10]. While x increases further from 0.40 to 0.85, the I_0 values of the alloy electrodes decrease, which can be ascribed to the fact that the surface electrocatalytic activity was decreased because of the diminution of the effective surface area [15] and the surface passivation was increased due to the increase of the oxide coverage [3,11,12].

Fig. 7 shows the Tafel polarization curves of the $La_{0.7}Mg_{0.3}Ni_{2.65}Mn_{0.1}Co_{0.75+x}$ (x = 0.00–0.85) alloy electrodes at 50% DOD and 298 K. The limiting current densities I_L obtained from these curves are listed in Table 2. It can be seen that, with increasing amount of Co addition, the I_L values of the alloy electrodes increase first and then decrease. When x = 0.30, the alloy electrode exhibits the largest I_L value (1912.0 mA/g). Thus, the effect of Co addition on the I_L is consistent with that on the HRD. In general, the limiting current density I_L represents the hydrogen diffusivity in the bulk of the alloys, that is, the larger the I_L value, the faster is the diffusion of the hydrogen atoms in the alloys [16]. In the present study, with increasing amount of Co addition, the variation of the I_L values of the alloy electrodes indicates that the hydrogen diffusion rate in the alloys increases first and then decreases.

3.4. Hydrogen diffusion behavior

The hydrogen diffusion coefficient D in the bulk of the alloy was also estimated by the potential-step method reported by Ura et al. [17]. Fig. 8 illustrates the semilogarithmic curves of the current–time response of the $La_{0.7}Mg_{0.3}Ni_{2.65}Mn_{0.1}Co_{0.75+x}$ (x = 0.00–0.85) alloy electrodes at fully charged state. As shown in Fig. 8, it is obvious that the value of log i immediately after the potential step decreases sharply with a decrease in concentration of the adsorbed hydrogen on the electrode surface due to the electro-oxidation. Thereafter, the value of log i decreases linearly because the rate-determining step changes from electro-oxidation to hydrogen diffusion in the alloy. From fitting the linear section for the current–time response curves as shown in Fig. 8, the hydrogen diffusion coefficient D of the alloy electrodes can be calculated by the following equation [18]:

$$\log i = \log\left(\frac{6FD}{da^2}\right)(C_0 - C_s) - \frac{\pi^2}{2.303}\frac{D}{a^2}t \quad (3)$$

in which i, D, C_0, C_s, a, d and t are the diffusion current density (A/g), the hydrogen diffusion coefficient (cm^2/s), the initial hydrogen concentration in the bulk of the alloy (mol/cm^3), the hydrogen concentration on the surface of the alloy particles (mol/cm^3), the alloy particle radius (cm), the density of the hydrogen storage alloy (g/cm^3), and the discharge time (s), respectively. According to Eq. (3) and using a = 13.12 μm, the D values of the alloy electrodes can be estimated and listed in Table 2. It can be seen that the D values of the

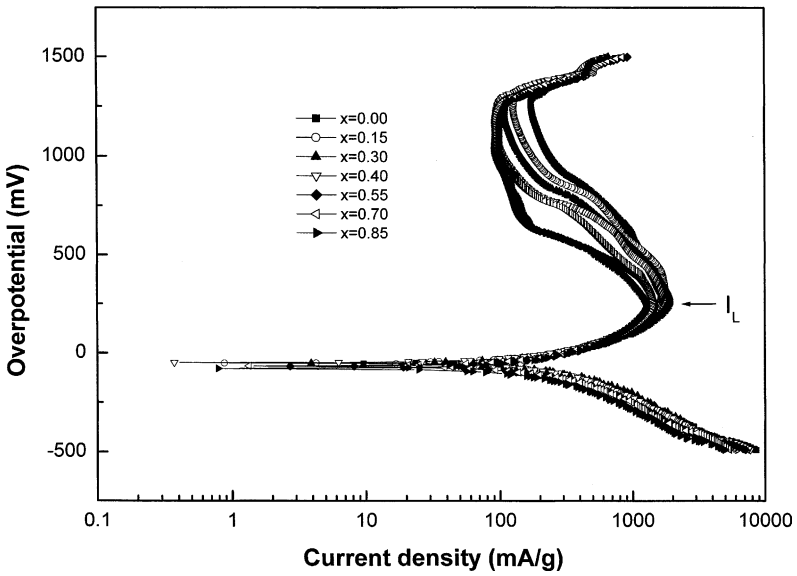

Fig. 7. Tafel polarization curves of the $La_{0.7}Mg_{0.3}Ni_{2.65}Mn_{0.1}Co_{0.75+x}$ (x = 0.00–0.85) alloy electrodes at 50% DOD and 298 K.

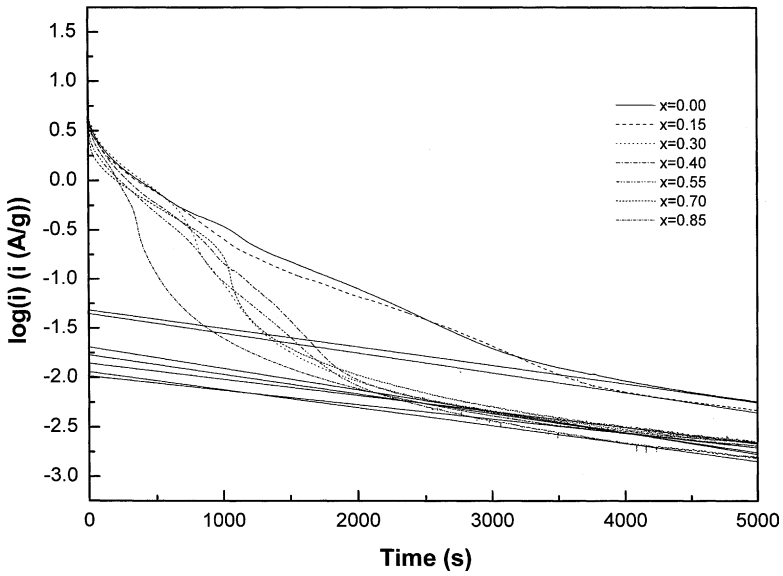

Fig. 8. Semilogarithmic curves of anodic current vs. time responses of the $La_{0.7}Mg_{0.3}Ni_{2.65}Mn_{0.1}Co_{0.75+x}$ (x = 0.00–0.85) alloy electrodes at fully charged state.

alloy electrodes increase first from 0.75×10^{-11} (x = 0.00) to 0.87×10^{-11} cm^2/s (x = 0.30) and then decrease to 0.58×10^{-11} cm^2/s (x = 0.85) with increasing amount of Co addition. The variation of the D values is in good agreement with that of the I_L values, which also indicates that the diffusion rate for hydrogen in the bulk of the alloys was accelerated first and then decreased.

Fig. 9 shows the response of discharge capacity vs. time after fully charged state of the $La_{0.7}Mg_{0.3}Ni_{2.65}Mn_{0.1}Co_{0.75+x}$ (x = 0.00–0.85) alloy electrodes with an applied + 600 mV potential step at 298 K. It is very obvious that the electrochemical capacities increase quickly at first and then slow down with time. Moreover, the total discharge capacities within 5000 s are reduced with increasing amount of Co addition. This result is consistent with the maximum discharge capacity measurement as listed in Fig. 1 and Table 1. It can also be noted that, within 500 s, the initial discharge rate of the alloy electrodes is accelerated first and then slowed down with the increase of Co addition. This fact also confirms the variation of the electrochemical kinetics of the alloy electrodes with increasing Co addition, that is, the electrochemical kinetics of the alloy electrodes increases first and then decreases. When

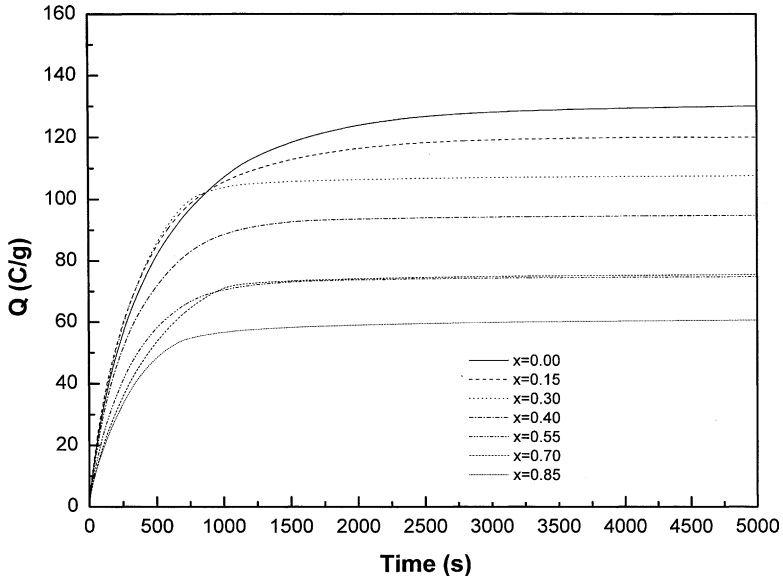

Fig. 9. Response of discharge capacity vs. time after fully charged state $La_{0.7}Mg_{0.3}Ni_{2.65}Mn_{0.1}Co_{0.75+x}$ (x = 0.00–0.85) alloy electrodes with an applied + 600 mV potential step at 298 K.

$x = 0.30$, the alloy electrode exhibits the best electrochemical kinetics.

4. Conclusions

The overall electrochemical performances were investigated by measuring the activation, the discharge capacity, the cyclic behavior, the high rate dischargeability (HRD), the electrochemical impedance spectra (EIS), the exchange current density I_0, the limiting current density I_L and the hydrogen diffusion coefficient D of the hydrogen storage alloys in the composition range of $La_{0.7}Mg_{0.3}Ni_{2.65}Mn_{0.1}Co_{0.75+x}$ ($x = 0.00$–0.85). The following conclusions can be drawn:

Increase in the amount of Co addition decreases the maximum discharge capacities of the alloy electrodes due to the relative change of the phase abundance of the (La, Mg)Ni_3 phase and the $LaNi_5$ phase in the alloys studied and the increase of the equilibrium pressure for hydrogen desorption.

The cyclic stability of the alloy electrodes was significantly improved with increasing amount of Co addition because of the relative lower value of V_H and the formation of protective oxides (hydroxides).

The HRDs of the alloy electrodes were increased by adding a proper amount of Co ($x \leq 0.30$), which can be ascribed to the formation of a Raney Ni–Co film with higher electrocatalytic activity resulting from the concentration of Ni and Co at the alloy surface. However, with further increasing Co addition, the HRDs of the alloy electrodes decrease because of the formation of $Co(OH)_2$ at the alloy surface. The investigations on the charge-transfer resistance at the surface R_{ct}, the exchange current density I_0, the limiting current density I_L and the diffusion coefficient of hydrogen in the alloys D also confirm the variation of the electrochemical kinetics of the alloy electrodes studied.

Acknowledgement

This work was supported by the National Natural Science Foundation of China (50131040).

References

[1] Y.F. Liu, H.G. Pan, M.X. Gao, R. Li, Y.Q. Lei, J. Alloys Compd. 387 (2004) 147.
[2] J.J.G. Willems, K.H.J. Buschow, J. Less-Common Met. 129 (1987) 13.
[3] T. Vogt, J.J. Reilly, J.R. Johnson, G.D. Adzic, J. McBreen, J. Electrochem. Soc. 146 (1999) 15.
[4] D. Chartouni, F. Meli, A. Züttel, K. Gross, L. Schlapbach, J. Alloys Compd. 241 (1996) 160.
[5] H. Oesterreicher, J. Clinton, H. Bittner, Mater. Res. Bull. 11 (1976) 1241.
[6] T. Takeshita, W.E. Wallace, R.S. Craig, Inorg. Chem. 13 (1974) 2282.
[7] G.D. Adzic, J.R. Johnson, S. Mukerjee, J. McBreen, J.J. Reilly, J. Alloys Compd. 253–254 (1997) 579.
[8] Y.F. Liu, H.G. Pan, M.X. Gao, R. Li, Y.Q. Lei, J. Alloys Compd., 2004, (in press).
[9] M.E. Fiorino, R.L. Opila, K. Konstadinidas, W.C. Fang, J. Electrochem. Soc. 143 (1996) 2422.
[10] Y. Choquette, H. Menard, L. Brossard, Int. J. Hydrogen Energy 15 (1990) 21.
[11] B.S. Haran, B.N. Popov, R.E. White, J. Electrochem. Soc. 145 (1998) 3000.
[12] A.B. Yuan, N.X. Xu, J. Alloys Compd. 322 (2001) 269.
[13] N. Kuriyama, T. Sakai, H. Miyamura, I. Uehara, H. Ishikawa, T. Iwasaki, J. Alloys Compd. 202 (1993) 183.
[14] P.H.L. Notten, P. Hokkeling, J. Electrochem. Soc. 138 (1991) 1877.
[15] C. Iwakura, K. Fukuda, H. Senoh, H. Inoue, M. Matsuoka, Y. Yamamoto, Electrochim. Acta 43 (1998) 2041.
[16] B.V. Ratnakumar, C. Witham, R.C. Bowman Jr., A. Hightower, B. Fultz, J. Electrochem. Soc. 143 (1996) 2578.
[17] H. Ura, T. Nishina, I. Uchida, J. Electroanal. Chem. 396 (1995) 169.
[18] G. Zhang, B.N. Popov, R.E. White, J. Electrochem. Soc. 142 (1995) 2695.